Published in final edited form as:

Oncogene. 2018 February 15; 37(7): 924–934. doi:10.1038/onc.2017.395.

Nutrient sensor O-GlcNAc transferase controls cancer lipid metabolism via SREBP-1 regulation

Valerie L. Sodi[1], **Zachary A. Bacigalupa**[1], **Christina M. Ferrer**[1], **Joyce V. Lee**[2], **Wiktoria A. Gocal**[1], **Dimpi Mukhopadhyay**[1], **Kathryn E. Wellen**[2], **Mircea Ivan**[3], and **Mauricio J. Reginato**[1,4]

[1]Department of Biochemistry and Molecular Biology, Drexel University College of Medicine, Philadelphia, PA 19102, USA

[2]Department of Cancer Biology, Abramson Family Cancer Research Institute, University of Pennsylvania Perelman School of Medicine, Philadelphia, PA 19104, USA

[3]Department Medicine, Indiana University, Indianapolis, IN 46202, USA

Abstract

Elevated O-GlcNAcylation is associated with disease states such as diabetes and cancer. O-GlcNAc transferase (OGT) is elevated in multiple cancers and inhibition of this enzyme genetically or pharmacologically inhibits oncogenesis. Here we show that O-GlcNAcylation modulates lipid metabolism in cancer cells. OGT regulates expression of the master lipid regulator the transcription factor sterol regulatory element binding protein 1 (SREBP-1) and its transcriptional targets both in cancer and lipogenic tissue. OGT regulates SREBP-1 protein expression via AMP Activated protein kinase (AMPK). SREBP-1 is critical for OGT-mediated regulation of cell survival and of lipid synthesis, as overexpression of SREBP-1 rescues lipogenic defects associated with OGT suppression, and tumor growth *in vitro* and *in vivo*. These results unravel a previously unidentified link between O-GlcNAcylation, lipid metabolism and the regulation of SREBP-1 in cancer and suggests a crucial role for O-GlcNAc signaling in transducing nutritional state to regulate lipid metabolism.

Keywords

O-GlcNAc; OGT; cancer; lipid metabolism; SREBP-1; FAS; ACLY; lipogenesis

Increased glycolytic flux observed in cancer cells, termed the Warburg effect (1), feeds not only glycolysis but other glucose dependent pathways as well, such as the Pentose Phosphate Pathway (PPP) and the Hexosamine Biosynthetic Pathway (HBP). HBP diverts

[4]Address Correspondence to: Mauricio J. Reginato, Ph.D., Drexel University College of Medicine, Department of Biochemistry and Molecular Biology, 245 N. 15th Street. Philadelphia, Pennsylvania, Phone: (215) 762-3554, FAX: (215) 762-4452, Mauricio.Reginato@drexelmed.edu.

Conflict of Interest

The authors declare no conflict of interest.

fructose-6-phosphate from glycolysis to produce UDP-GlcNAc that acts as the amino sugar donor to O-linked β-N-acetylglucosamine (O-GlcNAc) transferase (OGT) (2, 3). This enzyme is responsible for the addition of GlcNAc moieties to select serine and threonine residues of nuclear and cytosolic proteins involved in a wide variety of cellular functions. This reversible modification is analogous to phosphorylation (4) and cycles through addition by OGT and removal by the glycoside hydrolase O-GlcNAcase (OGA). O-GlcNAcylation can modulate a proteins function by altering stability, localization, protein-protein interaction, phosphorylation status, and/or DNA binding ability (5) and is known to occur on a variety of proteins associated with oncogenesis and tumor progression including c-Myc, AKT and NF-κB (6–8). Alterations in OGT and O-GlcNAc have been found to be associated with several pathologies such as diabetes, cardiovascular disease, neurodegeneration and more recently cancer (9, 10). Both O-GlcNAcylation and OGT levels are commonly increased in cancer and reduction of OGT and O-GlcNAcylation in cancer cells results in decreased growth and metastasis *in vivo* (11) (12) (13).

Increasing evidence indicates that cancer cells display specific alterations in pathways that drive lipogenesis to support membrane synthesis and generate signaling molecules required for rapid cell growth (14). Most normal adult tissues obtain lipids from the bloodstream in the form of dietary free fatty acids, however, cancer cells employ *de novo* lipogenesis (15). *De-novo* lipogenesis is a critical process to sustain growth and survival in cancer cells (14). This consists of activation and expression of enzymes involved in generating lipids, such as; fatty acid synthase (FAS), acetyl-CoA carboxylase (ACC), and ATP-citrate lyase (ACLY) as well as a transcription factor responsible for regulating these enzymes, the sterol regulatory element binding protein (SREBP-1) (16). The SREBP-1c and SREBP-2 transcription factors are known to regulate many proteins involved in lipid and cholesterol synthesis, respectively, while the SREBP-1α isoform is an activator of all SREBP-responsive genes (17). SREBP family transcription factors are synthesized as inactive precursors that reside in the endoplasmic reticulum membrane and nuclear envelope. Upon decreases in sterol or lipid levels, (18) these proteins are bound by SREBP-cleavage activating protein (SCAP) and proteolytically cleaved generating an N-terminal region containing the basic helix-loop-helix–leucine zipper for DNA binding (17). Mature SREBPs can then enter the nucleus and regulate target gene promoters. SREBP-1 overexpression has been found in many cancers including breast (19) (20) and targeting SREBP-1 in cancer cells resulted in significant cell death *in vitro* and slowed tumor growth *in vivo* (21) demonstrating its importance in contributing to cancer phenotypes and survival.

AMP- activated protein kinase (AMPK) is an important metabolic sensor that is implicated in cancer growth and survival (22). AMPK activation occurs in response to a variety of cellular stressors including low glucose and depletion of ATP levels. Downstream of AMPK, mTOR and other drivers of cellular growth are directly phosphorylated to inhibit their synthetic actions within cells to ration energy and substrates. AMPK directly regulates lipid metabolism in hepatic, muscle and adipose tissue through phosphorylation of SREBP-1 and ACC (23, 24). Its tumor suppressive role is well documented in a variety of cancers through its regulation of mTOR, ACC and inflammation (25); however a direct connection to SREBP-1 in cancer has not yet been established.

Here, we demonstrate a connection between nutrient sensor O-GlcNAcylation, SREBP-1 and lipid synthesis in cancer. Our results show that OGT and O-GlcNAcylation are required for lipid synthesis in breast cancer cells through the regulation of SREBP-1 in an AMPK-dependent manner. OGTs regulation of cancer growth and survival requires lipids and SREBP-1 expression as restoring SREBP-1 expression in the context of OGT inhibition prevented cancer cell growth *in vitro* and restored tumor growth *in vivo*. Thus, O-GlcNAcylation serves to link cancer cell nutritional status to lipid metabolism and cell growth via regulation of SREBP1.

Results

O-GlcNAcylation regulates lipid metabolism in breast cancer cells

To understand the impact of O-GlcNAcylation on cancer metabolism, global metabolomics analysis using liquid chromatography-mass spectrometry (LC-MS) was utilized to investigate the effect of OGT reduction on metabolites in triple-negative MDA-MB-231 human breast cancer cells. MDA-MB-231 cells containing OGT RNAi for 48 hours (Fig. 1A) demonstrated statistically significant ($p<0.05$) changes in 124 out of 301 metabolites examined when compared to control RNAi cells (Fig. S1, Supplementary Table 1). There were 35 biochemicals elevated while 89 reduced in OGT knockdown cancer cells compared to controls (Supplementary Table 1). KEGG pathway analysis identified a number of metabolic pathways that were significantly altered in cancer cells depleted of OGT. Reducing OGT in MDA-MB-231 cells elevated pathways associated with biosynthesis of alkaloids, reductive carboxylate cycle and TCA cycle while reducing metabolites associated with aminoacyl-tRNA biosynthesis, ABC transporters, biosynthesis of unsaturated fatty acids, pantothenate/CoA biosynthesis and fatty acid biosynthesis (Fig. 1B).

One of the largest changes in metabolites was in lipids. Of the lipid metabolites measured, 43% significantly decreased following OGT inhibition, compared to decreases in 27% of the measured amino acids, decreases in 21% of the carbohydrate metabolites and 14% of nucleotides (Fig. 1C). Levels of free fatty acids, including the polyunsaturated fatty acid linoleate that cannot be generated by mammalian cells, decreased significantly in shOGT-treated cells compared to control cells (Fig. S2). Similar to free fatty acids, several lysolipids and a number of long chain fatty acids were reduced in shOGT cells, as compared to control at 48 hrs (Fig. S2). In response to OGT inhibition, decreased free fatty acid pools may result in reduced phospholipid synthesis and/or increased fatty acid mobilization from phospholipids resulting in the observed decrease in lysolipids at 48 hrs. To confirm metabolomics profiling results, we measured free fatty acids in MDA-MB-231 cells and found a ~50% decrease in free fatty acid levels in OGT knockdown cells compared to control cells (Fig. 2A). We found a similar reduction of free fatty acid levels in the breast cancer cell lines MCF-7 (Fig. S3A, 3B) and SUM-159 (Fig. S4A, 4B) expressing OGT RNAi compared to control cells. In addition, cancer cells MDA-MB-231 (Fig. 2B) and MCF-7 (Fig. S3C) also contained lower levels of intracellular lipid droplets as measured by nile red staining (26). Conversely, overexpression of OGT in MCF-7 cells (Fig. 2C) significantly increased free fatty acid levels (Fig. 2D) and nile red staining (Fig. S2D) compared to control cells. Treatment of MDA-MB-231 cells with the OGT pharmacological

inhibitor Ac-5sGlcNAc also resulted in a significant decrease in free fatty acids (Fig. S5A) and lipid droplets (Fig. S5B). To determine if lipids contribute to OGT-mediated phenotypes on cell growth, we treated MDA-MB-231 cells stably expressing OGT RNAi with exogenous lipids palmitate/oleic acid. Treatment with exogenous lipids partly rescued growth defects resulting from OGT suppression (Fig. S5C) and reduced levels of apoptotic marker cleaved PARP (Fig. S5D). Thus, O-GlcNAcylation regulates levels of lipid metabolites and free fatty acids and this regulation contributes to growth in breast cancer cells.

O-GlcNAcylation regulates transcription factor SREBP-1 and lipid enzymes in breast cancer cells and lipogenic tissue

To examine whether O-GlcNAcylation may regulate lipid metabolism via critical regulator of lipid metabolism SREBP-1, we first examined whether expression of SREBP-1, OGT and global O-GlcNAcylation change as mammary tumors progress in a spontaneous breast cancer model *in vivo*. We utilized tissue from the MMTV-PyMT transgenic breast cancer mouse model where mammary hyperplasia can be detected as early as 4 weeks and a large percentage of mice developed carcinoma at ~14 weeks (27) (Fig. S6A). Protein expression of OGT and O-GlcNAcylation levels increased notably from week 8 to 12 during progression in this tumor model as well as nuclear SREBP-1 protein (N) levels and its transcriptional target ACLY (Fig. S6B). Consistent with increased SREBP-1 expression, nile red staining was increased in MMTV-PyMT derived mammary gland at week 8 compared to a wildtype mouse mammary gland of the same background (Fig. S6C).

To directly examine whether O-GlcNAcylation regulates SREBP-1 and lipogenic enzymes in breast cancer cells, we targeted OGT both genetically and pharmacologically. Inhibition of OGT via RNAi in breast cancer cells MDA-MB-231 (Fig. 3A), MCF7 (Fig. S3A), and SUM159 (Fig. S4A) results in decreased protein expression of both the ER transmembrane precursor (P) and the cleaved nuclear transcription factor form of SREBP-1 (N). Consistent with a decrease in SREBP-1 expression, OGT inhibition resulted in decreased protein expression of SREBP-1 transcriptional targets ACLY and FAS in MDA-MB-231 (Fig. 3A), MCF-7 (Fig. S3A) and SUM-159 (Fig. S4A) breast cancer cell lines. MDA-MB-231 cells stably expressing OGT RNAi also contain decreased levels of mRNA of SREBP-1 transcriptional targets FAS, ACLY, ELOVL7 (ELOVL Fatty Acid Elongase 7), ACC and LPL (Lipoprotein Lipase) compared to controls (Fig. 3B). Pharmacological inhibition of OGT using Ac-5sGlcNAc resulted in reduced total O-GlcNAcylation and similar decreases in SREBP-1 and FAS in MBA-MB-231 cells (Fig. 3C). Conversely, overexpression of OGT in MCF-7 cells increased SREBP-1 protein levels (Fig. 3D, Fig. S3E) as well as levels of ACLY and FAS (Fig. 3D). To further examine a functional connection between OGT and lipid biosynthesis, we performed a Gene Essentiality similarity analysis on the breast cancer cell lines for which this type of data is publicly available (CCLE/Achilles Project). The 7,500 genes for which essentiality score are available were ranked based on their similarity with OGT's score, using the nearest neighbor analysis publicly available. Critical components of lipid synthesis were among the top correlated genes with OGT including SREBP-1 transcriptional targets (28) ACACB (Acetyl-CoA carboxylase 2), MHGCS1 (Hydroxymethylglutaryl-CoA synthase), ACSL6 (Long chain Acyl-CoA synthetase 6), and

ACLY (Fig. S6D). This result suggests that breast cancer cells exhibiting higher dependency on OGT are generally more dependent on lipid biosynthesis, providing unbiased and independent support to the functional connection between OGT and this biosynthetic pathway.

Since *de novo* lipogenesis also occurs in lactating mammary glands (29), we examined whether OGT could regulate SREBP-1 and lipids in lactating breast tissue from mice containing *ogt* floxed alleles. We injected adenoviral (Ad)-Cre recombinase or Ad-GFP as control into the mammary fat pads of lactating female mice containing *ogt* exons flanked by loxP recombination sites (30). Injecting Ad-Cre to lactating mammary fat pad resulted in reduced OGT protein expression and O-GlcNAcylation as well as reduced SREBP-1 and ACLY protein levels compared to Ad-GFP treated mice as shown in immunoblot analysis (Fig. S7A). Moreover, targeting OGT in lactating breast reduced nile red staining which correlates with reduced SREBP-1 and FAS protein compared to Ad-GFP treated mice via immunohistochemical analysis (Fig. S7B). Consistent with reduced fatty acids in mammary tissue, growth of pups nursed by Ad-Cre treated dams was significantly attenuated and average litter weight was reduced when comparing growth rate over time to control pups (Fig. S7C). Thus, OGT and O-GlcNAcylation regulates SREBP-1, its transcriptional targets and lipid metabolism in breast cancer cells and lipogenic tissue.

O-GlcNAcylation regulates SREBP-1 expression in a proteasomal and AMPK-dependent manner

We next examined the mechanism by which OGT and O-GlcNAcylation regulates SREBP-1 in cancer cells. SREBP-1 protein can be regulated by proteasomal degradation (31) thus we examined whether O-GlcNAc regulation is proteasomal-dependent. Treatment of breast cancer cells with proteasomal inhibitor MG132 blocked the OGT suppression-induced decrease in nuclear SREBP-1, and to a lesser extent precursor SREBP-1 compared to control (Fig. S8A) and reversed decreases in SREBP-1 transcriptional target ACLY (Fig. S8A). SREBP-1 is regulated by the tumor suppressor and E3-ubiquitin ligase FBW7 (31), thus we examine whether reducing O-GlcNAcylation altered SREBP-1 interaction with FBW7. Reducing OGT expression led to increased interaction between SREBP-1 and FBW7, as indicated by coimmunoprecipitation experiments in breast cancer cells (Fig. S8B) and HEK-293 cells overexpressing FLAG-tagged SREBP (Fig. S8C). Consistent with the idea that OGT regulates SREBP-1 via the proteasomal pathway, we detected a two-fold increase in SREBP-1 ubiquitination under conditions of decreased OGT levels in HEK-293 cells compared to controls (Fig. S8C). Indeed, we show that FBW7 is partly required for OGT regulation of SREBP-1 as stable knockdown of FBW7 in MDA-MB-231 cells partly reverses OGT shRNA mediated inhibition of SREBP-1 protein levels (Fig. S8D). SREBP-1 does not appear to be directly O-GlcNAcylated as immunoprecipitation of exogenous SREBP-1 contained no detectable O-GlcNAcylation when compared to a known target of OGT (data not shown). This does not rule out the possibility that SREBP-1 is O-GlcNAc modified but suggests that O-GlcNAcylation may regulate SREBP-1 protein stability indirectly.

We have previously demonstrated that reduction of OGT via RNAi, in breast cancer cells, results in metabolic stress and leads to activation of the AMPK pathway (32). AMPK is activated under low nutrient conditions and is known to phosphorylate SREBP-1 on Ser372 and inhibit its cleavage and maturation in hepatocytes (24). Thus we examined whether OGT may regulate SREBP-1 in an AMPK-dependent manner. Reducing O-GlcNAcylation in breast cancer cells leads to an increase in phosphorylated AMPK (T172) (Fig. 4A). Using a phospho-antibody that recognizes SREBP-1 phosphorylation on Ser372, we observe an increase in SREBP-1 phosphorylation when OGT is suppressed in MDA-MB-231 cells, correlating with activation of AMPK as measured by phosphorylation at T172 (Fig. 4A). We tested the requirement of AMPK in OGT-mediated changes in SREBP-1 in MDA-MB-231 cells by treating cells with the AMPK inhibitor Compound C. MDA-MB-231 cells treated with Compound C contained decreased AMPK activation as measured by phosphorylation of its substrate Raptor-(Ser792) compared to control cells (Fig. 4B). Phosphorylation of SREBP-1 on Ser372 was reduced in Compound C treated cells and the reduced SREBP-1 and ACLY protein levels observed upon suppression of OGT were partly reversed by treatment with Compound C (Fig. 4B, Fig. S8E). Similar results were obtained in MDA-MB-157 cells with Compound C (data not shown) and using dorsomorphin 2HCL (Fig. S8F) in MDA-MB-231 cells suggesting that OGT regulation of SREBP-1 is AMPK-dependent in multiple breast cancer cells. We then assessed whether regulation of SREBP-1 by OGT required AMPK using WT and AMPK-/- mouse embryonic fibroblasts (MEFs). In WT MEFs, OGT inhibition results in decreased SREBP-1 protein expression and transcriptional targets ACLY (Fig. 4C). However, AMPK null MEFs showed reduced change in SREBP-1, ACLY protein expression upon OGT inhibition compared to control MEFs. To determine whether OGT regulation of AMPK and SREBP-1 is dependent on changes in metabolism, we tested whether treating OGT depleted cells with methyl-pyruvate, a permeable nutrient that supports mitochondrial bioenergetics (33), would reverse AMPK activation and SREBP-1 levels. Reducing OGT levels in MDA-MB-231 cells leads to activation of AMPK and increased phosphorylation of SREBP-1 and reduced total levels of SREBP-1 and transcriptional target FAS (Fig. 4D). However, SREBP-1 phosphorylation was reduced and SREBP-1 total levels and FAS levels were restored in OGT-depleted cells treated with methyl-pyruvate compared to control cells (Fig. 4D) suggesting OGT regulation of SREBP-1 is dependent on metabolic changes. Taken together, these results suggest that O-GlcNAcylation regulates SREBP-1 protein levels, its interaction with E3 ligase FBW7 and, is in part, AMPK-dependent and associated with O-GlcNAcylation regulation of cell metabolism.

O-GlcNAcylation-mediated cancer cell survival requires SREBP-1 regulation of lipid and glucose metabolism in cancer cells

To determine if changes in SREBP-1 were required for the lipid defects observed upon OGT inhibition, we overexpressed exogenous SREBP-1 to restore levels in the context of OGT knockdown. While exogenous SREBP-1 nuclear protein levels were still affected by OGT suppression in cells, they were comparable to levels in control cells thereby ensuring that SREBP-1 had been restored to basal levels (Fig. 5A, Fig. S9A). Cells stably overexpressing exogenous SREBP-1 restored nile red staining (Fig. 5B) and significantly restored free fatty acid levels (Fig. 5C) in OGT knockdown cells to levels similar to control cells. In addition,

overexpression of SREBP-1 rescued protein levels of transcriptional targets FAS and ACLY in OGT knockdown cells compared to controls (Fig. 5A). We next tested whether regulation of SREBP-1 by OGT played a role in cancer cell growth. Growth inhibition resulting from OGT suppression as shown by crystal violet staining (Fig. 5D) and anchorage-independent growth (Fig. 5E, Fig. S9B) was partially reversed when SREBP-1 was overexpressed in OGT knockdown MDA-MB-231 cells. Apoptotic factors such as cleaved caspase 3, which are induced upon OGT suppression, were no longer activated in SREBP-1 overexpressing cells compared to controls and the loss of anti-apoptotic Bcl2 was prevented in these cells (Fig. S9C).

We noticed that SREBP-1 overexpression rescued growth to a much greater extent (Fig. 5D) when compared to addition of exogenous lipids in OGT knockdown cells (Fig. S5C). Since we have previously shown that OGT regulates HIF-1α and its transcriptional target GLUT1, and overexpression of a HIF-1α stable mutant or GLUT1 can also partly rescue OGT knockdown phenotypes (32), we examined expression of HIF-1α and GLUT1 in SREBP-1 overexpressing cells. In cells overexpressing SREBP-1 we did not detect any changes in HIF-1α. However, surprisingly, we found maintenance of GLUT1 in OGT knockdown cells (Fig. 6A). Consistent with the idea that SREBP-1 overexpression may be regulating GLUT1 function, we found that inhibition of glucose consumption caused by OGT-knockdown was reversed in SREBP-1 overexpressing cells (Fig. 6B). Similar reversal was seen in lactate production suggesting that SREBP-1 can also regulate OGT-mediated glycolytic flux (Fig. 6C). SREBP-1 overexpression also reversed metabolic signaling including decreases in mTOR signaling seen with OGT suppression in control cells, as measured by phosphorylated 4EBP-1 and S6 ribosomal protein (Fig. 6A). Downstream of mTOR, c-Myc protein expression was also rescued by SREBP-1 overexpression (Fig. 6A). Thus, O-GlcNAc regulation of SREBP-1 in cancer cells is critical for lipid metabolism but also for regulation of glycolytic flux and metabolic signaling in a HIF1-independent manner.

SREBP-1 is critical for OGT-mediated regulation of breast cancer tumorigenesis *in vivo*

To determine if the regulation of SREBP-1 by OGT was important for tumor growth and survival *in vivo*, we employed an orthotopic xenograft animal model. We injected MDA-MB-231- Luciferase cells either stably expressing control shRNA or OGT shRNA in the presence or absence of SREBP-1 overexpression (Fig. 7A) orthotopically into the inguinal fat pad of female Nu/Nu mice. We monitored tumor growth as readout of bioluminescence intensity and using caliper measurements. Reducing OGT levels in MDA-MB-231 cells blocks tumor growth in vivo (Fig. 7B) (11). However, cells overexpressing SREBP-1 partly rescued the effects of OGT depletion in cancer cells in vivo (Fig. 7B). At animal endpoint we observed a significant rescue of tumor volume in SREBP-1 overexpressing cells in the context of OGT depletion compared to control OGT depleted cells (Fig. 7C). Thus, OGT regulation of tumor growth in vivo is partly dependent on SREBP-1 expression and function.

Discussion

Cancer cells generate nearly all fatty acids via de novo synthesis to support rapid tumor growth and survival (21). In this study, we demonstrate that O-GlcNAcylation, elevated in

nearly all cancers (10), is required and sufficient to control SREBP function and lipid metabolism in cancer cells. We show that O-GlcNAcylation, via metabolic control of AMPK signaling, regulates SREBP-1 phosphorylation and stability as well as its transcriptional targets ACLY and FAS to regulate lipid metabolism and cancer cell growth and survival (Fig. 7D). Our study uncovers the critical function of O-GlcNAcylation in controlling lipid metabolism in tumor cells linking OGT regulation of metabolism to AMPK signaling and SREBP regulation. Thus, elevated O-GlcNAcylation not only maintains aerobic glycolysis in cancer cells (32), but also maintains lipid metabolism via regulation of SREBP independent of OGT regulation of HIF-1α. Additionally, we find that O-GlcNAcylation also regulates lipid metabolism and SREBP in adult lipogenic tissue such as lactating mammary gland and suggest cancer cells have co-opted this normal regulation of de novo lipid synthesis.

O-GlcNAcylation has been shown to regulate key transcription factors that directly bind to promoters of a number of metabolic enzymes including c-Myc (34), HIF-1α (32) and now SREBP-1. These transcription factors allow for coordinate up- and down-regulation of entire metabolic processes associated with the Warburg effect in cancer cells (35). C-Myc has been shown to be directly O-GlcNAcylated on threonine 58 (36) and increase its protein stability. Consistent with these studies, reducing OGT and O-GlcNAcylation reduces protein levels of c-Myc. Surprisingly, overexpression of SREBP-1 restored c-Myc protein levels in OGT depleted cells suggesting that SREBP-1 regulation of c-Myc overrides it regulation by O-GlcNAcylation. This, along with reversing GLUT1 expression, may explain why overexpression of SREBP-1 partly restores glucose and lactate levels in OGT-depleted cells. Importantly, SREBP-1 restoration of metabolic defect and mTOR signaling was independent of regulation of HIF-1α. Recent studies suggest that SREBP-2 can regulate stem cell-like properties in prostate cancer cells in part via transcriptional activation of c-Myc (37). Thus, SREBP-1 may regulate c-Myc by direct binding or through other mechanisms and suggests that SREBP-1 may have broader functions beyond lipid synthesis regulation in cancer cells.

Although the requirement of lipogenesis has been well chronicled in a variety of cancer tissues, inhibition of this process as a means of therapy has proved challenging. Genetic inhibition of lipogenesis downstream of SREBP-1 favors the use of inhibitors against enzymes such as FAS and ACLY for the treatment of cancer. More recently, the FAS inhibitor TVB-2640 which carries a more favorable tolerability (38), entered phase I clinical trials for solid malignant tumors (21). OGT inhibitors have not yet been tested in animal studies. However, since targeting OGT regulates three key transcriptional regulators of cancer metabolism, including c-Myc, HIF-1α, and SREBP-1, it suggest that these compounds may provide strong anti-tumor effects especially in highly metabolic cancers. Thus, targeting OGT in cancer may serve as a therapeutic alternative to directly targeting enzymes such as FAS or ACLY in breast cancer and other lipid-dependent cancers as well.

Materials and Methods

Reagents

MG132, Nile Red, Methyl-pyruvate were purchased from Sigma-Aldrich (St. Louis, MO, USA). Compound C and Dorsomorphin (2HCL) from Selleck-Chemicals (Houston, TX,

USA). Ac-5sGlcNAc was provided by D. Vocadlo (Simon Fraser University). Antibodies used were Anti-OGT, Anti-O-GlcNAc, Anti-FLAG from Sigma-Aldrich; Anti-pSREBP1-(S372), Anti-pAMPK-(T172), Anti-pRaptor-(S792), Anti-pS6 Ribosomal Protein-(S240/244), Anti-p4EBP1-(T70), Anti-AMPK, Anti-Raptor, Anti-S6 Ribosomal Protein, Anti-4EBP1, Anti-FAS, Anti-ACC, Anti-Ubiquitin, Anti-Cleaved Caspase 3, Anti-Cleaved PARP from Cell Signaling (Danvers, MA, USA); Anti-Actin, Anti-Bcl2 from Santa Cruz Biotechnology; Anti-SREBP1, Anti-HIF1α, Anti-c-MYC from Novus Biologicals; Anti-SREBP1, Anti-ACLY, Anti-Glut1 from Abcam; Anti-FBW7 from Bethyl Labs. pLKO.FLAG-SREBP1 (Addgene-32017 from D. Sabatini).

Cell Culture

MDA-MB-231 and MCF-7 cells were obtained from ATCC and cultured following instructions. SUM-159 and MDA-MB-157 cells were a generous gift from T. Seagroves (U Tennessee). WT and AMPKα1/α2 KO MEFs were provided by B Viollet (INSERM) (23). shRNA sequences and lentiviral particles were generated as previously described (11). pSicoR-shFBW7 was kindly provided by L. Busino (University of Pennsylvania) and previously described (39).

Western blotting

Western blotting procedures were carried out as previously described (40).

Animal experiments

Athymic nude Nu/Nu 5–6 week old female mice (Charles River, Wilmington, MA, USA) were inoculated with 1.5×10^6 MDA-MB-231 cells stably expressing luciferase and either pBabe-Control or plko-SREBP-1 as well as either Control or OGT shRNA. Cells were injected in 100 μl of 1x PBS containing 20% matrigel (Invitrogen) using a 271/2-gauge needle into the fourth-inguinal mammary fat pad and imaged as previously described (32). Tumor volumes were calculated as V=(length)x(width)2 ×0.52. All protocols using animals were approved by the Institutional Animal Care and Use Committee at Drexel University. B6.129-Ogttm1Gwh/J female mice have been previously described (30) and obtained as a gift from S Jones (University of Louisville) (30). Mice were injected into the mammary fat pad with Ad5-CMV-GFP or Ad5-CMV-Cre (2.7 × 107 PFU, from the Baylor University) as previously described (13) post parturition daily for three days. Histology was performed as previously described (12).

Free Fatty Acid Quantification

Free Fatty Acids were quantified using the Fatty Acid Kit from Biovision as per the manufacturers' instructions. Equal number of cells from each sample were used for quantification of lipids using a choloform/1% TritonX solution. Cells were centrifuged and the lipid-containing layer was dried. Lipids were resuspended and acyl-CoA derivatives were generated using kit provided enzyme. Colormetric detection was performed in a Synergy HT plate reader (BIO-TEK Instruments Inc.).

Metabolite Analysis

Metabolomic Analysis of MDA-MB-231 cells stably expressing Control or OGT shRNA for 48 hrs was performed as described previously (32). Welch's t-tests were performed to compare data between experimental groups. Multiple comparisons were accounted for by estimating the false discovery rate using q-values. Pathway enrichment analysis was performed by independently subjecting significantly increased and decreased metabolites identified through Metabolon Analysis to MBRole2.0 software (41). Enrichment results are ranked by FDR corrected p-values. All KEGG pathway results with p-value <0.05 are shown.

Immunoprecipitation

Assays were performed as described previously (40).

qRT-PCR

qRT-PCR was performed as previously described (40). Taqman primer probes for OGT (Hs00914634_g1), SREBF-1 (Hs1088691-m1), ACLY (Hs00982738-m1), FASN (Hs0105622-m1), ACACA (Hs01046047-m1), ELOVL7 (Hs00405151-m1), LPL (Hs00173425-m1) and Cyclophilin A (Hs99999904_m1) were purchased from Applied Biosystems (Foster City, CA, USA).

Metabolic Assays

For glucose uptake, cells were plated at a density of 100,000 cells/well. After 48 hours, media was collected and cells were counted using the Guava Easy Cyte Plus system and CytoSoft (Millipore Corporation). Control media and each sample were measured on Accu-chek Active (Roche). Glucose consumption was calculated by subtracting sample measurement from control and normalizing to cell number. Lactate assay were performed as previously described (32).

Nile Red Staining of Cells and Tissue

Cells or tissues were fixed using 4% Formalin, washed in 1xPBS prior to staining with 5μg/ml Nile Red solution and incubated for 30 minutes. Samples were then washed in PBS and photographed on EVOS FL (Life technologies) using Texas-Red filter.

Statistical Analysis

All results shown are of at least three independent experiments and shown as averages and presented as mean ± s.e. *P*-values were calculated using a Student's two-tailed test (* represents at least $P\text{-value} \leq 0.05$ or as marked in figure legend). Statistical analysis of growth rate of mice was performed using ANCOVA.

Supplementary Material

Refer to Web version on PubMed Central for supplementary material.

Acknowledgments

We thank Nicholas Xerri for technical support and Mignon Keaton for help in analyzing LC-MS metabolite data. This work was supported by NCI grants CA192868 (to V.L.S.), CA183574 (to C.M.F.), and CA155413 (to M.J.R.).

References

1. Boroughs LK, DeBerardinis RJ. Metabolic pathways promoting cancer cell survival and growth. Nat Cell Biol. 2015 Apr; 17(4):351–9. [PubMed: 25774832]
2. Hart GW, Housley MP, Slawson C. Cycling of O-linked beta-N-acetylglucosamine on nucleocytoplasmic proteins. Nature. 2007 Apr 26; 446(7139):1017–22. [PubMed: 17460662]
3. Wellen KE, Thompson CB. Cellular metabolic stress: considering how cells respond to nutrient excess. Mol Cell. 2010 Oct 22; 40(2):323–32. [PubMed: 20965425]
4. Varki, A., Cummings, R., Esko, J., et al. Essentials of Glycobiology. Cold Spring Harbor, NY: Cold Spring Harbor Laboratory Press; 1999. The O-GlcNAc Modification.
5. Ozcan S, Andrali SS, Cantrell JE. Modulation of transcription factor function by O-GlcNAc modification. Biochim Biophys Acta. 2010 May-Jun;1799(5–6):353–64. [PubMed: 20202486]
6. Chou TY, Dang CV, Hart GW. Glycosylation of the c-Myc transactivation domain. Proc Natl Acad Sci U S A. 1995 May 9; 92(10):4417–21. [PubMed: 7753821]
7. Kawauchi K, Araki K, Tobiume K, Tanaka N. Loss of p53 enhances catalytic activity of IKKbeta through O-linked beta-N-acetyl glucosamine modification. Proc Natl Acad Sci U S A. 2009 Mar 3; 106(9):3431–6. [PubMed: 19202066]
8. McClain DA, Lubas WA, Cooksey RC, Hazel M, Parker GJ, Love DC, et al. Altered glycan-dependent signaling induces insulin resistance and hyperleptinemia. Proc Natl Acad Sci U S A. 2002 Aug 6; 99(16):10695–9. [PubMed: 12136128]
9. Hardiville S, Hart GW. Nutrient regulation of signaling, transcription, and cell physiology by O-GlcNAcylation. Cell metabolism. 2014 Aug 5; 20(2):208–13. [PubMed: 25100062]
10. Ferrer CM, Sodi VL, Reginato MJ. O-GlcNAcylation in Cancer Biology: Linking Metabolism and Signaling. J Mol Biol. 2016 Aug 14; 428(16):3282–94. [PubMed: 27343361]
11. Caldwell SA, Jackson SR, Shahriari KS, Lynch TP, Sethi G, Walker S, et al. Nutrient sensor O-GlcNAc transferase regulates breast cancer tumorigenesis through targeting of the oncogenic transcription factor FoxM1. Oncogene. 2010 May 13; 29(19):2831–42. [PubMed: 20190804]
12. Lynch TP, Ferrer CM, Jackson SR, Shahriari KS, Vosseller K, Reginato MJ. Critical role of O-Linked beta-N-acetylglucosamine transferase in prostate cancer invasion, angiogenesis, and metastasis. J Biol Chem. 2012 Mar 30; 287(14):11070–81. [PubMed: 22275356]
13. Ferrer CM, Lu TY, Bacigalupa ZA, Katsetos CD, Sinclair DA, Reginato MJ. O-GlcNAcylation regulates breast cancer metastasis via SIRT1 modulation of FOXM1 pathway. Oncogene. 2017 Jan 26; 36(4):559–69. [PubMed: 27345396]
14. Baenke F, Peck B, Miess H, Schulze A. Hooked on fat: the role of lipid synthesis in cancer metabolism and tumour development. Dis Model Mech. 2013 Nov; 6(6):1353–63. [PubMed: 24203995]
15. Swinnen JV, Brusselmans K, Verhoeven G. Increased lipogenesis in cancer cells: new players, novel targets. Curr Opin Clin Nutr Metab Care. 2006 Jul; 9(4):358–65. [PubMed: 16778563]
16. Santos CR, Schulze A. Lipid metabolism in cancer. FEBS J. 2012 Aug; 279(15):2610–23. [PubMed: 22621751]
17. Horton JD, Goldstein JL, Brown MS. SREBPs: transcriptional mediators of lipid homeostasis. Cold Spring Harb Symp Quant Biol. 2002; 67:491–8. [PubMed: 12858575]
18. Walker AK, Jacobs RL, Watts JL, Rottiers V, Jiang K, Finnegan DM, et al. A conserved SREBP-1/phosphatidylcholine feedback circuit regulates lipogenesis in metazoans. Cell. 2011 Nov 11; 147(4):840–52. [PubMed: 22035958]
19. Beckner ME, Fellows-Mayle W, Zhang Z, Agostino NR, Kant JA, Day BW, et al. Identification of ATP citrate lyase as a positive regulator of glycolytic function in glioblastomas. Int J Cancer. 2010 May 15; 126(10):2282–95. [PubMed: 19795461]

20. Li W, Tai Y, Zhou J, Gu W, Bai Z, Zhou T, et al. Repression of endometrial tumor growth by targeting SREBP1 and lipogenesis. Cell Cycle. 2012 Jun 15; 11(12):2348–58. [PubMed: 22672904]
21. Rohrig F, Schulze A. The multifaceted roles of fatty acid synthesis in cancer. Nat Rev Cancer. 2016 Sep.:23.
22. Luo Z, Zang M, Guo W. AMPK as a metabolic tumor suppressor: control of metabolism and cell growth. Future Oncol. 2010 Mar; 6(3):457–70. [PubMed: 20222801]
23. Laderoute KR, Amin K, Calaoagan JM, Knapp M, Le T, Orduna J, et al. 5′-AMP-activated protein kinase (AMPK) is induced by low-oxygen and glucose deprivation conditions found in solid-tumor microenvironments. Mol Cell Biol. 2006 Jul; 26(14):5336–47. [PubMed: 16809770]
24. Li Y, Xu S, Mihaylova MM, Zheng B, Hou X, Jiang B, et al. AMPK phosphorylates and inhibits SREBP activity to attenuate hepatic steatosis and atherosclerosis in diet-induced insulin-resistant mice. Cell Metab. 2011 Apr 6; 13(4):376–88. [PubMed: 21459323]
25. Zadra G, Batista JL, Loda M. Dissecting the Dual Role of AMPK in Cancer: From Experimental to Human Studies. Molecular cancer research : MCR. 2015 Jul; 13(7):1059–72. [PubMed: 25956158]
26. Greenspan P, Mayer EP, Fowler SD. Nile red: a selective fluorescent stain for intracellular lipid droplets. J Cell Biol. 1985 Mar; 100(3):965–73. [PubMed: 3972906]
27. Guy CT, Cardiff RD, Muller WJ. Induction of mammary tumors by expression of polyomavirus middle T oncogene: a transgenic mouse model for metastatic disease. Mol Cell Biol. 1992 Mar; 12(3):954–61. [PubMed: 1312220]
28. Eberle D, Hegarty B, Bossard P, Ferre P, Foufelle F. SREBP transcription factors: master regulators of lipid homeostasis. Biochimie. 2004 Nov; 86(11):839–48. [Review]. [PubMed: 15589694]
29. Anderson SM, Rudolph MC, McManaman JL, Neville MC. Key stages in mammary gland development. Secretory activation in the mammary gland: it's not just about milk protein synthesis! Breast Cancer Res. 2007; 9(1):204. [PubMed: 17338830]
30. O'Donnell N, Zachara NE, Hart GW, Marth JD. Ogt-dependent X-chromosome-linked protein glycosylation is a requisite modification in somatic cell function and embryo viability. Mol Cell Biol. 2004; 24:1680–90. [PubMed: 14749383]
31. Sundqvist A, Bengoechea-Alonso MT, Ye X, Lukiyanchuk V, Jin J, Harper JW, et al. Control of lipid metabolism by phosphorylation-dependent degradation of the SREBP family of transcription factors by SCF(Fbw7). Cell Metab. 2005 Jun; 1(6):379–91. [PubMed: 16054087]
32. Ferrer CM, Lynch TP, Sodi VL, Falcone JN, Schwab LP, Peacock DL, et al. O-GlcNAcylation regulates cancer metabolism and survival stress signaling via regulation of the HIF-1 pathway. Mol Cell. 2014 Jun 5; 54(5):820–31. [PubMed: 24857547]
33. Buzzai M, Bauer DE, Jones RG, Deberardinis RJ, Hatzivassiliou G, Elstrom RL, et al. The glucose dependence of Akt-transformed cells can be reversed by pharmacologic activation of fatty acid beta-oxidation. Oncogene. 2005 Jun 16; 24(26):4165–73. [PubMed: 15806154]
34. Itkonen HM, Minner S, Guldvik IJ, Sandmann MJ, Tsourlakis MC, Berge V, et al. O-GlcNAc transferase integrates metabolic pathways to regulate the stability of c-MYC in human prostate cancer cells. Cancer Res. 2013 Aug 15; 73(16):5277–87. [PubMed: 23720054]
35. Shaw RJ, Cantley LC. Decoding key nodes in the metabolism of cancer cells: sugar & spice and all things nice. F1000 Biol Rep. 2012; 4:2. [PubMed: 22242042]
36. Chou TY, Hart GW, Dang CV. c-Myc is glycosylated at threonine 58, a known phosphorylation site and a mutational hot spot in lymphomas. J Biol Chem. 1995; 270:18961–5. [PubMed: 7642555]
37. Li X, Wu JB, Li Q, Shigemura K, Chung LW, Huang WC. SREBP-2 promotes stem cell-like properties and metastasis by transcriptional activation of c-Myc in prostate cancer. Oncotarget. 2016 Mar 15; 7(11):12869–84. [PubMed: 26883200]
38. Buckley D, Heuer T, O'Farrell M, McCulloch B, Kemble G. Translational studies of a first−in−class FASN Inhibitor, TVB−2640, linking preclinical studies to clinical laboratory observations in solid tumor patients. Molecular Cancer Research. 2016; 14(Suppl 1) Abstr. A75.
39. Busino L, Millman SE, Scotto L, Kyratsous CA, Basrur V, O'Connor O, et al. Fbxw7alpha- and GSK3-mediated degradation of p100 is a pro-survival mechanism in multiple myeloma. Nat Cell Biol. 2012 Mar 04; 14(4):375–85. [PubMed: 22388891]

40. Sodi VL, Khaku S, Krutilina R, Schwab LP, Vocadlo DJ, Seagroves TN, et al. mTOR/MYC Axis Regulates O-GlcNAc Transferase Expression and O-GlcNAcylation in Breast Cancer. Mol Cancer Res. 2015 May; 13(5):923–33. [PubMed: 25636967]

41. Lopez-Ibanez J, Pazos F, Chagoyen M. MBROLE 2.0-functional enrichment of chemical compounds. Nucleic Acids Res. 2016 Jul 08; 44(W1):W201–4. [PubMed: 27084944]

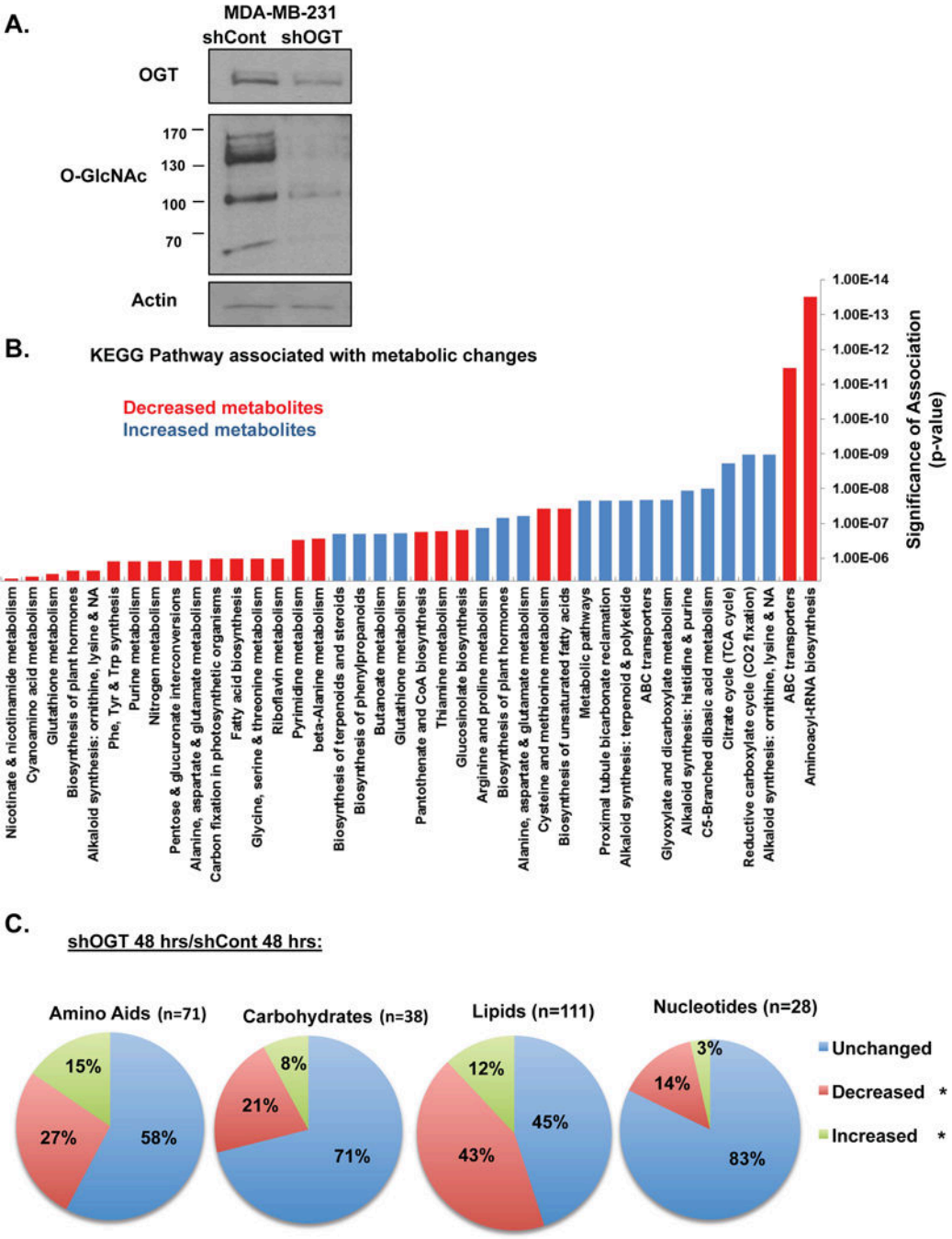

Figure 1. Metabolomics Profiling of MDA-MB-231 breast cancer cells with stable OGT suppression

(A) Cell lysates from MDA-MB-231 cells stably expressing control or OGT shRNA were collected for immunoblot analysis with the indicated antibodies and used for liquid chromatography-mass spectrometry (LC-MS) metabolomics profiling. (B) KEGG pathways highly associated metabolic changes resulting from OGT suppression. Pathways association with significantly increased metabolites (blue) and significantly decreased metabolites (red) are displayed in ranking p-values. Analysis was performed using MBrole2.0. (C) Pie graph showing metabolic categories altered in cells expressing OGT shRNA compared to control

shown. Data are represented as statistically significant ($p<0.05$) changes in 124 out of 301 metabolites, grouped by metabolites related to amino acids, carbohydrates, lipids and nucleotides.

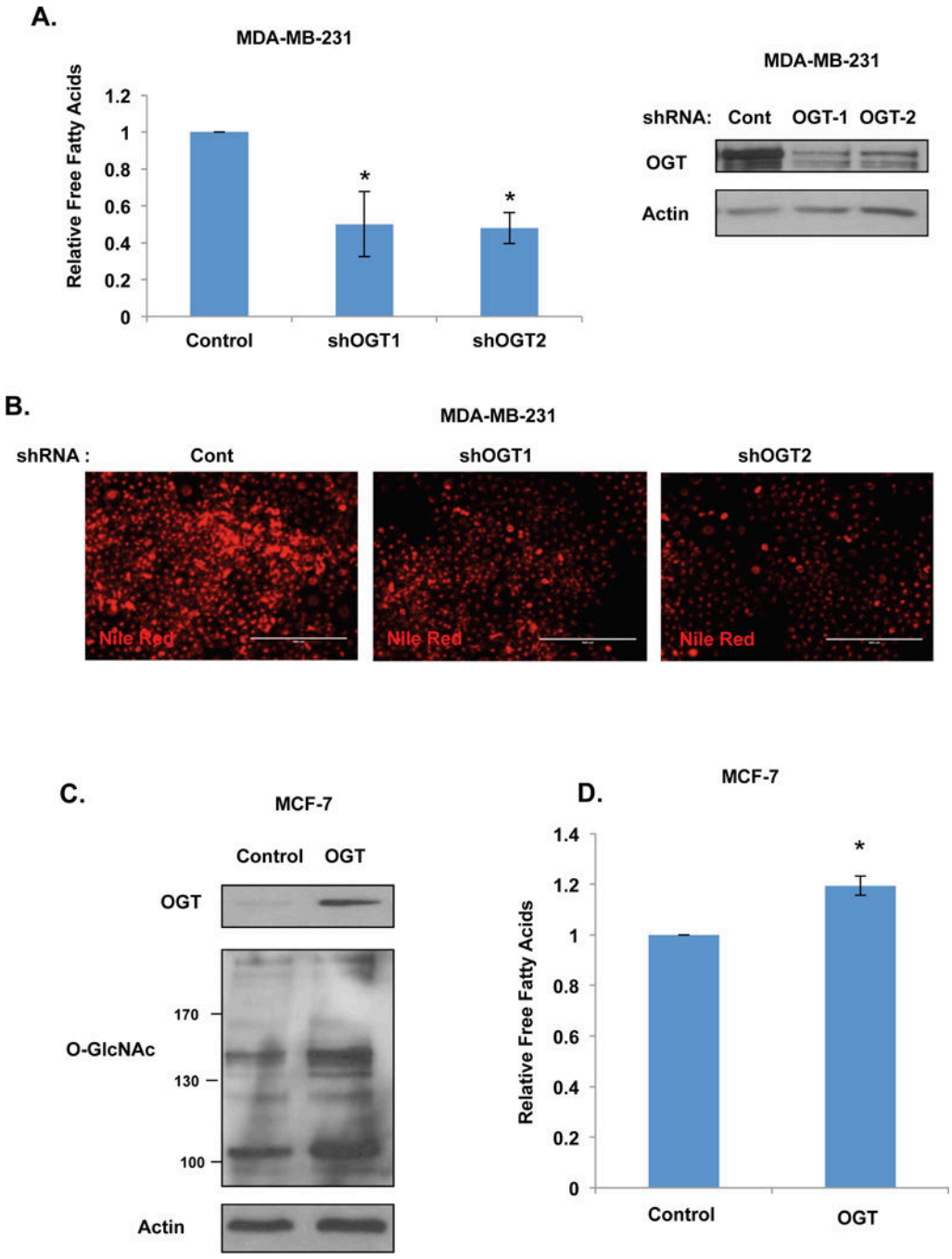

Figure 2. OGT Regulates Lipid Metabolism in Breast Cancer Cells

(A) Relative free fatty acids levels in MDA-MB-231 cells stably expressing control, OGT-1 or OGT-2 shRNA. Equal number of cells was analyzed in each sample and normalized to control. (B) Cell lysates from MDA-MB-231 cells expressing control, OGT-1 or OGT-2 shRNA were collected for immunoblot analysis with the indicated antibodies (B) Representative images of nile red staining of MDA-MB-231 cells under the same conditions as (A). (C) Cell lysates from MCF7 cells stably overexpressing control or Flag-OGT were

collected for immunoblot analysis with indicated antibodies. (D) Measurement of relative free fatty acids in MCF7 stably overexpressing control or Flag-OGT. Mean ± SE. *p<0.05.

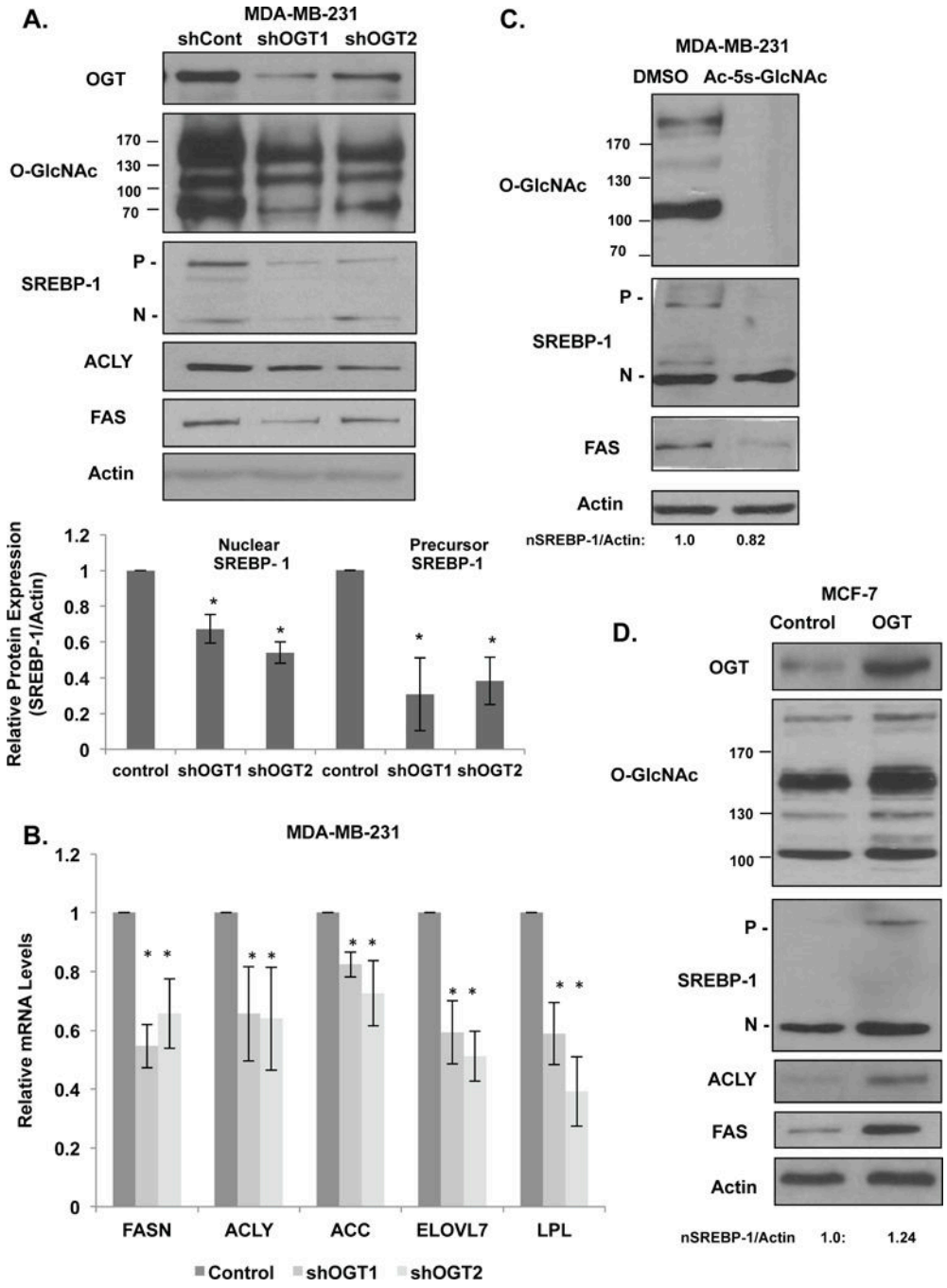

Figure 3. O-GlcNAcylation regulates expression of SREBP-1 and its transcriptional targets

(A) Cell lysates from MDA-MB-231 cells expressing control, OGT-1 or OGT-2 shRNA were collected for immunoblot analysis with the indicated antibodies (top). SREBP-1 protein expression quantified normalized to actin (below). (B). Measurement of relative mRNA expression of SREBP-1 target genes from control or stable OGT shRNA expressing MDA-MB-231 cells using qRT-PCR. All expression is normalized to cyclophilin A internal control and to MDA-MB-231 control samples. (C) Cell lysates from MDA-MB-231 cells treated for 48 hours with control (DMSO) or 100 μM Ac-5sGlcNAc for 48 hrs were

collected for immunoblot analysis with the indicated antibodies. (D) Cell lysates from MCF7 cells stably overexpressing control or Flag-OGT were collected for immunoblot analysis with indicated antibodies. Mean ± SE. *p<0.05 **p< 0.01.

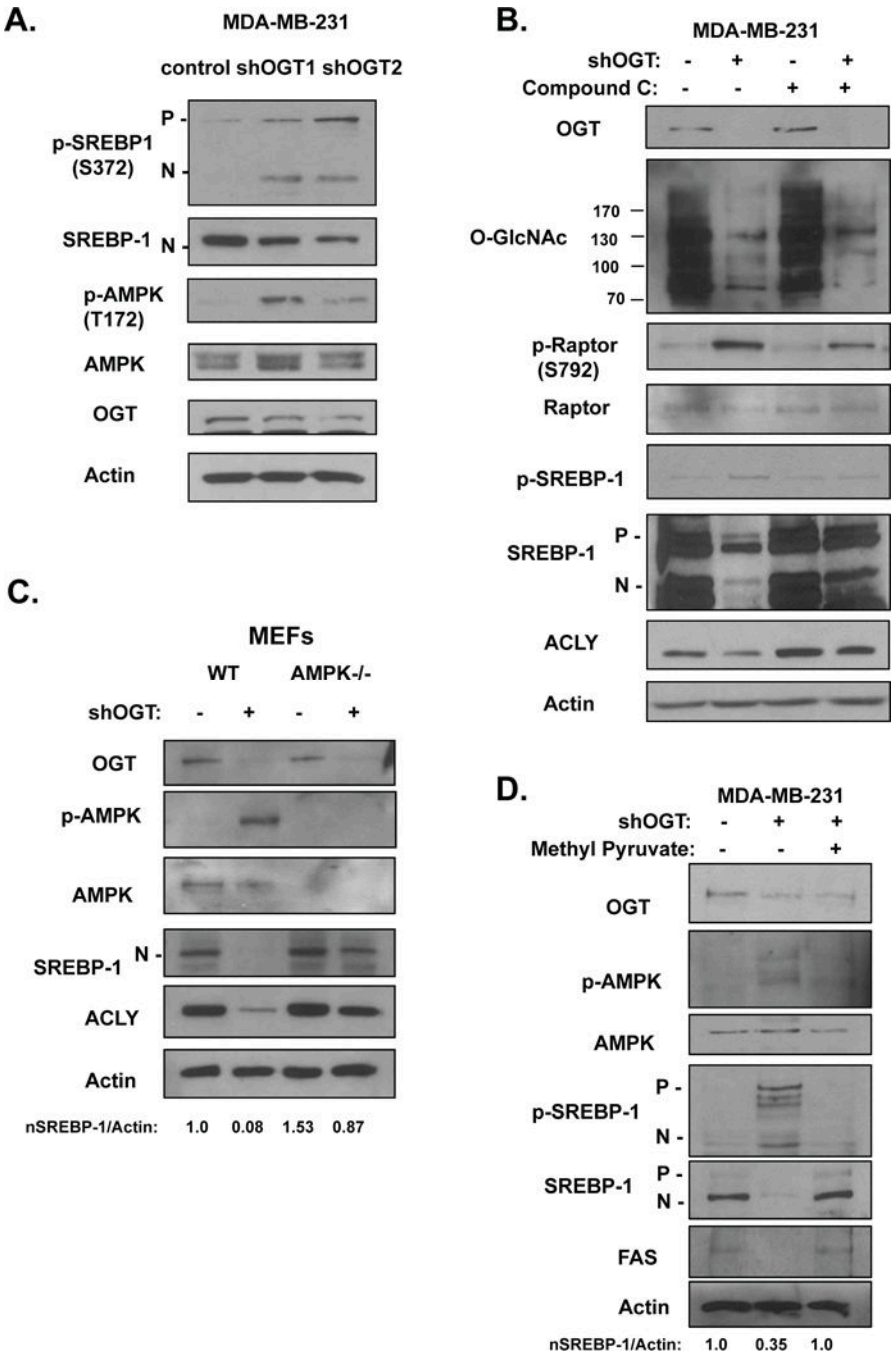

Figure 4. O-GlcNAcylation regulation of SREBP-1 is dependent on AMPK activation

(A) Cell lysates from MDA-MB-231 cells expressing control, OGT-1 or OGT-2 shRNA were collected for immunoblot analysis with the indicated antibodies. (B) Protein immunoblot of lysates from MDA-MB-231 expressing control or OGT shRNA and treated with vehicle (DMSO) or 10 μM Compound C for 24 hours, analyzed with the indicated antibodies. (C) Cell lysates from WT or AMPK -/- MEF cells expressing control or OGT shRNA were analyzed with the indicated antibodies by immunoblot (top). Quantification of SREBP-1 protein expression normalized to actin (below). (D) Cell lysates from MDA-

MB-231 cells expressing control or OGT shRNA treated with control (dH_20) or 10 μM methyl-pyruvate for 24 hours were collected and analyzed with the indicated antibodies. Mean ± SE. *$p<0.05$.

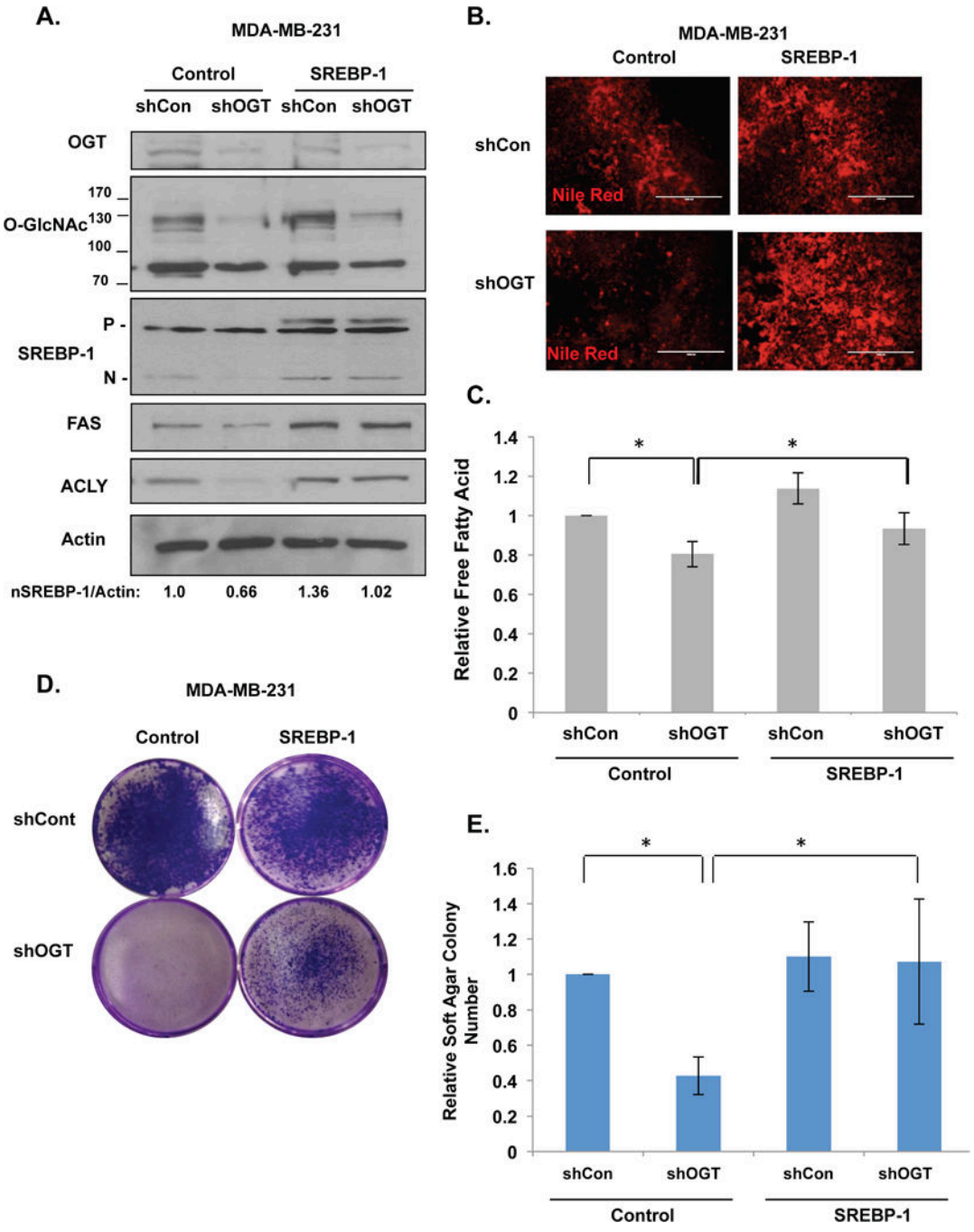

Figure 5. OGT-suppression induced decreases in lipids and cell growth are prevented when SREBP-1 expression is restored

(A) Cell lysates were collected from MDA-MB-231 cells were treated with control or OGT shRNA after stable infection with control or SREBP-1. Lysates were analyzed with the indicated antibodies (top). Quantification of relative SREBP-1 protein expression normalized to actin is displayed below panel. (B) Representative immunofluorescent imaging of nile red stained cells corresponding to the conditions in (A). (C) Quantification of measurements of relative free fatty acids within cells corresponding to the conditions in (A). (D) MDA-MB-231 cells were treated with control or OGT shRNA after stable infection

with control or SREBP-1 and cell colonies were stained with crystal violet. (E) Quantification of soft agar colony forming assays corresponding to conditions in (A-D) after staining with INT for visualization. Mean ± SE. *p<0.05.

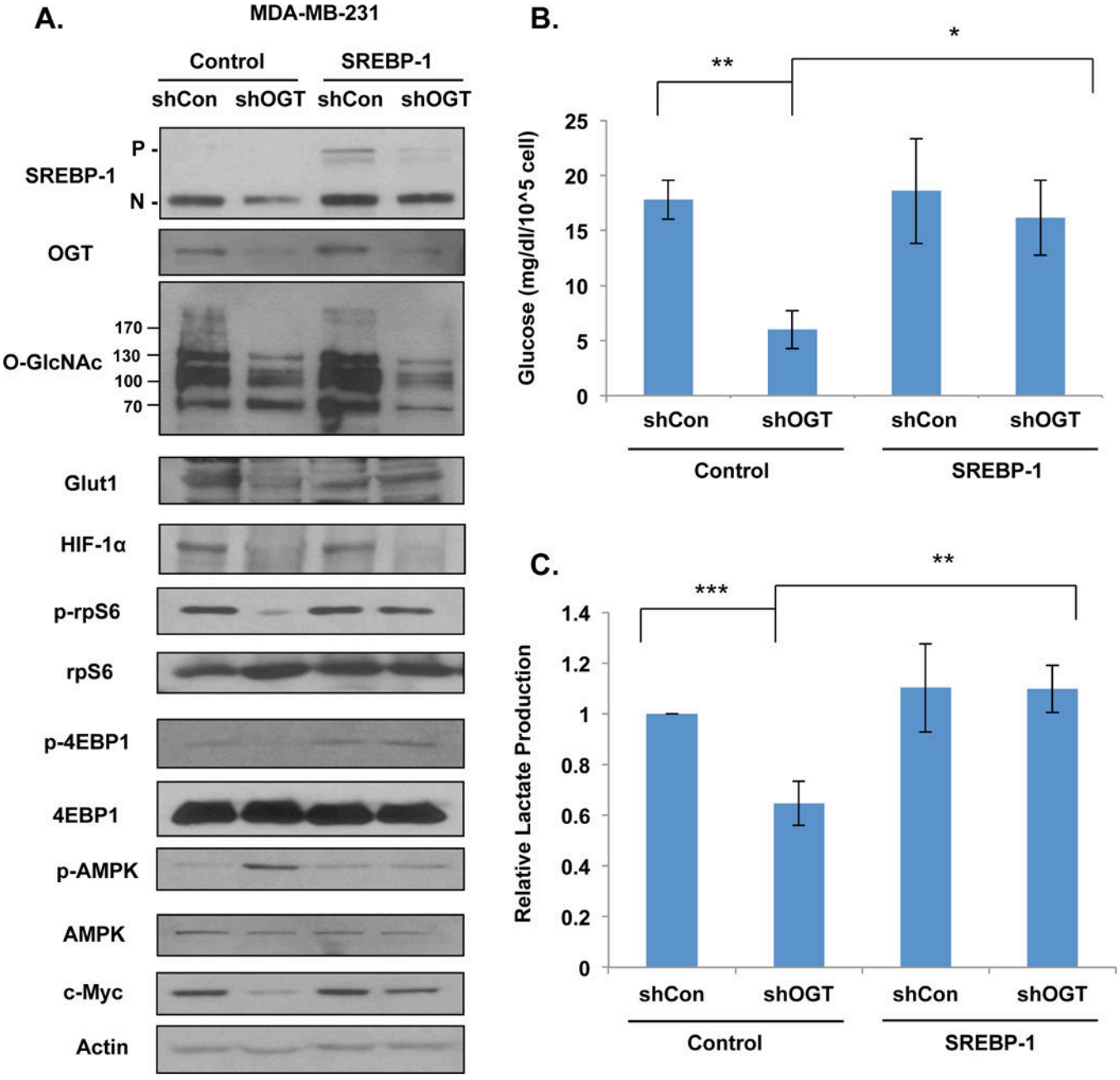

Figure 6. SREBP-1 restoration prevents OGT-suppression mediated decreases in mTOR signaling, activation of AMPK and decreased glycolytic regulators

(A) Cell lysates were collected from MDA-MB-231 cells were treated with control or OGT shRNA after stable infection with control or SREBP-1 and analyzed with the indicated antibodies. (B) Changes in lactate levels were measured from cells in (A) and normalized to control-treated cells. (C) Relative glucose consumption were measured from cells in (A) and normalized to cell number. Mean ± SEM. *p<0.05, **p<0.01.

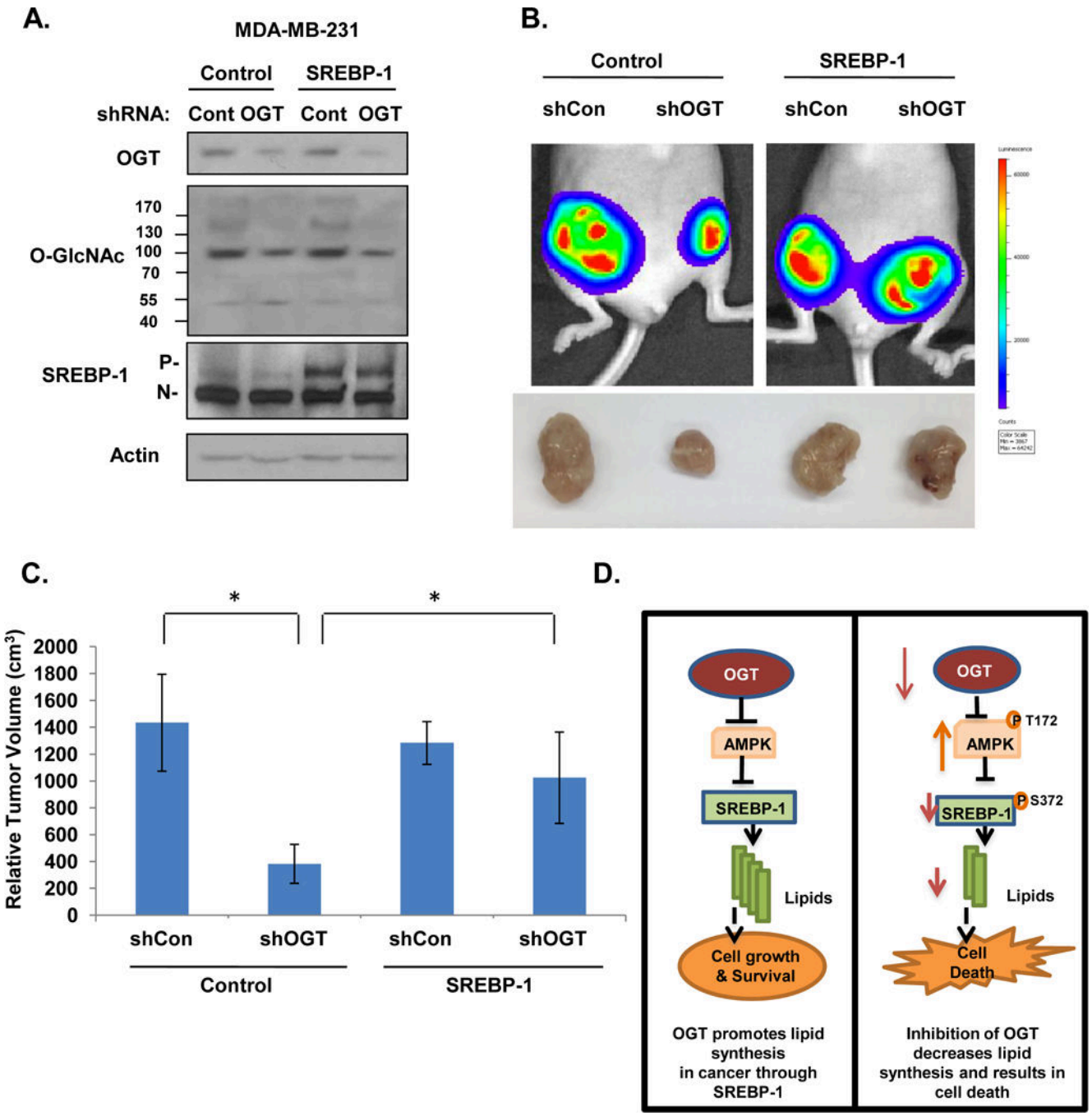

Figure 7. Decreased tumor growth *in vivo* by OGT suppression is partially rescued by SREBP-1 overexpression

(A) Cell lysates were collected prior to injection into mice from MDA-MB-231-Luciferase cells treated with control or OGT shRNA after stable infection with control or SREBP-1 and analyzed by immunoblot with the indicated antibodies. (B) Representative bioluminescent images of xenograft conditions corresponding to conditions in (A) from week 4–6 post-injection (endpoint as dictated by IACUC. (C) Mean tumor volume (mm^3) from MDA-MB-231 cells with the indicated treatment (as in A-B) (n=6/group). Mean ± SE. *p<0.05. (D) A schematic illustration of proposed model, showing OGT regulation of SREBP-1

protein and phosphorylation via regulation of AMPK that regulates lipid metabolism and cancer growth and survival.